Matched-Pair Comparison of ^{68}Ga-PSMA-11 PET/CT and ^{18}F-PSMA-1007 PET/CT: Frequency of Pitfalls and Detection Efficacy in Biochemical Recurrence After Radical Prostatectomy

Isabel Rauscher[1], Markus Krönke[1], Michael König[1], Andrei Gafita[1], Tobias Maurer[2,3], Thomas Horn[2], Kilian Schiller[4], Wolfgang Weber[1], and Matthias Eiber[1]

[1]Department of Nuclear Medicine, Klinikum rechts der Isar, Technical University Munich, Munich, Germany; [2]Department of Urology, Klinikum rechts der Isar, Technical University Munich, Munich, Germany; [3]Department of Urology and Martini-Klinik, University of Hamburg-Eppendorf, Hamburg, Germany; and [4]Department of Radiation Oncology, Klinikum rechts der Isar, Technical University Munich, Munich, Germany

^{18}F-labeled prostate-specific membrane antigen (PSMA)–ligand PET has several principal advantages over ^{68}Ga-PSMA-11. The purpose of this retrospective study was to evaluate the frequency of non–tumor-related uptake and the detection efficacy comparing ^{68}Ga-PSMA-11 PET/CT and ^{18}F-PSMA-1007 PET/CT in recurrent prostate cancer (PC) patients. **Methods:** The study included 102 patients with biochemically recurrent PC after radical prostatectomy undergoing ^{18}F-PSMA-1007 PET/CT imaging. On the basis of various clinical variables, patients with corresponding ^{68}Ga-PSMA-11 PET/CT scans were matched. All PET/CT scans (n = 204) were reviewed by 1 nuclear medicine physician. First, all PET-positive lesions were noted. Then, lesions suspected of being recurrent PC were differentiated from lesions attributed to a benign origin on the basis of known pitfalls and information from CT. For each region, the SUV_{max} of the lesion with the highest PSMA-ligand uptake was noted. Detection rates were determined, and SUV_{max} was compared separately for ^{68}Ga-PSMA-11 and ^{18}F-PSMA-1007. **Results:** In total, ^{18}F-PSMA-1007 PET and ^{68}Ga-PSMA-11 PET revealed 369 and 178 PSMA-ligand–positive lesions, respectively. ^{18}F-PSMA-1007 PET revealed approximately 5 times more lesions attributed to a benign origin than did ^{68}Ga-PSMA-11 PET (245 vs. 52 lesions, respectively). The benign lesions most frequently observed were ganglia, unspecific lymph node, and bone lesions, at a rate of 43%, 31%, and 24% for ^{18}F-PSMA-1007 PET and 29%, 42%, and 27% for ^{68}Ga-PSMA-11 PET, respectively. The SUV_{max} of lesions attributed to a benign origin was significantly higher ($P <$ 0.0001) for ^{18}F-PSMA-1007 PET. Further, a similar number of lesions was attributed to recurrent PC (124/369 for ^{18}F-PSMA-1007 PET and 126/178 for ^{68}Ga-PSMA-11 PET). **Conclusion:** The number of lesions with increased PSMA-ligand uptake attributed to a benign origin is considerably higher for ^{18}F-PSMA-1007 PET than for ^{68}Ga-PSMA-11 PET. This finding indicates the need for sophisticated reader training emphasizing known pitfalls and reporting within the clinical context.

Received Apr. 10, 2019; revision accepted Jun. 12, 2019.
For correspondence or reprints contact: Isabel Rauscher, Department of Nuclear Medicine, Klinikum rechts der Isar der TUM, Munich, Ismaninger Strasse 22, 81675 Munich, Germany.
E-mail: isabel.rauscher@tum.de
Published online Jun. 28, 2019.

Key Words: genitourinary; oncology; PET/CT; PSMA; pitfalls; prostate cancer

J Nucl Med 2020; 61:51–57
DOI: 10.2967/jnumed.119.229187

Biochemical recurrence (BCR) represents a major concern for patients with prostate cancer (PC) who have undergone primary radical prostatectomy (RP) (*1*). The ability to localize the site and extent of recurrent PC is of the utmost importance for directing salvage therapy. However, conventional imaging techniques such as CT or MRI have limited sensitivity for detecting recurrent disease (*2*). The introduction of ^{68}Ga-prostate-specific membrane antigen (PSMA)–11 PET in 2012 led to significantly improved detection rates in the BCR setting. Various mainly retrospective studies have indicated superior detection efficacy compared with conventional imaging and choline-based PET, especially at low prostate-specific antigen (PSA) levels (*3*). Along with the rapid adoption of PSMA-ligand PET worldwide, there is an exponentially increasing number of published case series and reports describing an increased PET signal in ganglia or other benign lesions (e.g., Paget disease and thyroid adenoma), suggesting that PSMA-ligand PET is not as specific as initially thought (*4*).

Recently, ^{68}Ga-labeled PSMA ligands have increasingly been replaced by ^{18}F-labeled counterparts. There are some major principle advantages of radiofluorinated tracers over ^{68}Ga-labeled PSMA ligands such as longer half-life (110 vs. 68 min), centralized production and distribution leading to cost savings, the possibility of large-batch production (cyclotron-produced ^{18}F vs. generator-produced ^{68}Ga), and the lower positron energy of ^{18}F than of ^{68}Ga, potentially improving spatial resolution and reducing blurring effects. So far, published experience with ^{18}F-labeled PSMA ligands is limited and includes only small patient numbers. In a head-to-head comparison of 14 patients with recurrent PC, ^{18}F-DCFPyL PET/CT performed equally as well as ^{68}Ga-PSMA-11 PET/CT (*5*). A follow-up study from Dietlein et al. using PSA-adjusted BCR cohorts indicated that ^{18}F-DCFPyL was noninferior to ^{68}Ga-PSMA-11 and suggested an improved sensitivity of ^{18}F-DCFPyL in

the PSA range of 0.5–3.5 ng/mL (*6*). Most recently, ^{18}F-PSMA-1007 PET has been introduced into PC imaging. It exhibits rapid blood clearance but only minimal urinary excretion, yielding potential advantages for local tumor assessment, because high tracer retention in the bladder and ureters is known to impair image interpretation (*7–11*).

Thus, the purpose of this retrospective analysis was to assess potential differences in the frequency of non–tumor-related PSMA-ligand uptake and to compare detection efficacy of ^{68}Ga-PSMA-11 PET/CT and ^{18}F-PSMA-1007 PET/CT using matched-pair cohorts of patients in BCR after RPE.

MATERIALS AND METHODS

Patient Population

The study retrospectively included 102 patients (median age, 71 ± 8 y; range, 51–84 y) with BCR after RPE (median PSA value, 0.87 ng/mL; range, 0.20–13.59 ng/mL) imaged at our institution between August 2017 and February 2018 using ^{18}F-PSMA-1007 PET/CT. The matched cohort consisted of 102 patients (median age, 70 ± 7 y; range, 50–82 y) with BCR after RPE (median PSA value, 0.91 ng/mL; range, 0.18–30.00 ng/mL) who underwent ^{68}Ga-PSMA-11 PET/CT. These 2 cohorts were chosen from the institution's database on the basis of the following clinical parameters: Gleason score (6–7 vs. 8–10), PSA value at the time of PET (0.2–0.5 ng/mL, >0.5–1.0 ng/mL, or >1.0–2.0 ng/mL vs. >2 ng/mL), primary T stage (≤2 vs. ≥3), primary N stage (0 vs. 1), and androgen deprivation therapy within 6 mo before the examination (yes vs. no). The characteristics of the matched-pair cohorts are summarized in Table 1. All patients gave written informed consent to the anonymized evaluation and publication of their data. All reported investigations were conducted in accordance with the Helsinki Declaration and with national regulations. The retrospective analyses were approved by the Ethics Committee of the Technical University Munich (permits 257/18 S and 5665/13).

^{18}F-PSMA-11 and ^{68}Ga-PSMA-11 PET/CT

^{18}F-PSMA-1007 was synthesized as described previously (*9,12*). Reagent kits, unprotected PSMA-1007 precursor, and PSMA-1007 reference standard were obtained from ABX. ^{18}F-PSMA-1007 was given to patients via an intravenous bolus (mean, 325 ± 40 MBq; range, 248–453 MBq), with the PET acquisition starting at a mean (±SD) of 94 ± 22 min (range, 45–163 min) afterward. ^{68}Ga-PSMA-11 was synthesized as described previously by Eder et al. (*13*). ^{68}Ga-PSMA-11 was given to patients via an intravenous bolus (mean, 147 ± 27 MBq; range, 94–232 MBq), and the PET acquisition was started at a mean of 54 ± 7 min (range, 41–85 min) afterward. All patients were examined on a Biograph mCT scanner (Siemens Medical Solutions). A diagnostic CT scan was initially performed in the portal venous phase 80 s after intravenous injection of an iodinated contrast agent (Imeron 300; Bracco Imaging) and was followed by the PET scan. All patients received a diluted oral contrast agent (300 mg of Telebrix; Guerbet). The PET scans were acquired in 3-dimensional mode with an acquisition time of 3–4 min per bed position or 1.1–1.5 mm/s using flow technique. Emission data were corrected for randoms, dead time, scatter, and attenuation and were reconstructed iteratively using ordered-subsets expectation maximization (4 iterations, 8 subsets) followed by a postreconstruction smoothing gaussian filter (5 mm in full width at half maximum).

Image Analysis

One nuclear medicine physician reviewed both the ^{68}Ga-PSMA-11 scans and the ^{18}F-PSMA-1007 scans (total $n = 204$). First, all PSMA-ligand PET–positive lesions were noted and grouped as local recurrence, abdominopelvic lymph nodes (LNs), supradiaphragmatic LNs, bone, or others (e.g., lung or liver). In a second step, lesions suspected of being recurrent PC were differentiated from those that were probably benign (e.g., ganglia, unspecific LNs, or degenerative changes) on the basis of known pitfalls and information from CT. For each anatomic region, the SUV_{max} of the lesion with the highest PSMA-ligand uptake was noted both for lesions suspected of being recurrent PC and for lesions attributed to a benign origin. To estimate the influence of high activity retention in the bladder, the SUV_{max} of the urinary bladder was measured and the tumor-to-background ratio (TBR) for local recurrent lesions was calculated. In addition, the shortest distance between local recurrence and the bladder wall was measured in millimeters.

TABLE 1
Patient Characteristics

Characteristic	^{68}Ga-PSMA-11 PET	^{18}F-PSMA-1007 PET
Patients (*n*)	102	102
Age at PET/CT (y)		
Median ± SD	69 ± 7	70 ± 8
Range	50–82	51–84
Initial Gleason score		
6–7	63	63
8–10	39	39
Initial pathologic primary tumor stage		
≤pT2	46	46
≥pT3	56	56
Initial pathologic regional LN stage		
pN0	76	76
pN1	26	26
Additional ADT after RPE	24	24
PSA value before PET/CT (ng/mL)		
Median	0.91	0.87
Range	0.18–30.00	0.20–13.59
0.2–0.5	35	35
>0.5–1.0	20	20
>1.0–2.0	21	21
>2.0	26	26

ADT = androgen deprivation therapy.

Statistical Analysis

Statistical analyses were performed with MedCalc software (version 13.2.0, 2014). All quantitative data are expressed as mean ± SD. *P* values of less than 0.05 were considered significant. Detection rates were determined, and the SUV_{max} of the most probably benign and suspected-PC lesions were compared separately for ^{68}Ga-PSMA-11 PET/CT and ^{18}F-PSMA-1007 PET/CT using the Mann–Whitney *U* test.

RESULTS

Distribution and Localization of PSMA-Ligand–Positive Lesions Attributed to Benign Origin

In total, ^{68}Ga-PSMA-11 and ^{18}F-PSMA-1007 PET/CT revealed 178 and 369 lesions with focal PSMA-ligand uptake, respectively.

^{18}F-PSMA-1007 PET revealed 245 lesions attributed to a benign origin, compared with 52 lesions on ^{68}Ga-PSMA-11 PET (Fig. 1A). The SUV_{max} of lesions attributed to a benign origin was significantly higher ($P < 0.0001$) on ^{18}F-PSMA-1007 PET than on ^{68}Ga-PSMA-11 PET (median SUV_{max}, 5.3 [range, 3.0–42.7] vs. 4.4 [range, 2.8–7.5], respectively; Supplemental Table 1). The main sites of PSMA-ligand–positive lesions attributed to a benign origin were ganglia, unspecific LNs, and bone, at rates of 43%, 31%, and 24% for ^{18}F-PSMA-1007 and 29%, 42%, and 27% for ^{68}Ga-PSMA-11 PET, respectively. Uptake in soft-tissue lesions attributed to a benign origin was seen only rarely on either ^{68}Ga-PSMA-11 PET or ^{18}F-PSMA-1007 PET (2% each) (Fig. 1B; Table 2). Representative examples of ^{18}F-PSMA-1007–positive lesions attributed to a benign origin are shown in Figure 2. The number of cases of bone PSMA-ligand uptake that was most probably unspecific (being predominantly in the ribs) was substantially higher on ^{18}F-PSMA-1007 PET than on ^{68}Ga-PSMA-11 PET (36 vs. 6 lesions, respectively). Table 4 details the location of unspecific uptake in bone. A representative example of a patient with an unspecific bone uptake is shown in Figure 3.

Lesion Detection and Localization Attributed to Recurrent PC

A similar number of PSMA-ligand–positive lesions was attributed to recurrent PC (126 and 124 suspected lesions on ^{68}Ga-PSMA-11 PET and ^{18}F-PSMA-1007 PET, respectively). This resulted in a higher percentage of lesions attributed to recurrent PC for ^{68}Ga-PSMA-11 (70.8%, 126/178) than for ^{18}F-PSMA-1007 PET (33.6%, 124/369; Fig. 1A). On a patient basis, lesions suspected of being recurrent PC were detected in 82 patients both on ^{68}Ga-PSMA-11 PET/CT and on ^{18}F-PSMA-1007 PET/CT, resulting in an identical detection rate of 80.4%. The SUVs of suspected lesions were similar ($P = 0.816$) on ^{68}Ga-PSMA-11 PET and ^{18}F-PSMA-1007 PET (median SUV_{max}, 9.9 [range, 3.3–112.5] and 9.4 [range, 2.7–234.4], respectively; Supplemental Table 1 [supplemental materials are available at http://jnm.snmjournals.org]).

The main sites for lesions attributed to recurrent PC on ^{68}Ga-PSMA-11 PET versus ^{18}F-PSMA-1007 PET were, respectively, abdominopelvic LNs in 34% versus 29%, local recurrence in 26% versus 22%, supradiaphragmatic LNs in 17% versus 27%, bone metastases in 21% versus 18%, and other soft-tissue metastases in 2% versus 4% (Table 3). TBR was significantly higher ($P < 0.0001$) on ^{18}F-PSMA-1007 PET (median TBR, 2.50; range, 0.77–19.70) than on ^{68}Ga-PSMA-11 PET (median TBR, 0.99; range, 0.11–10.39). Notably, local recurrence detected on ^{18}F-PSMA-1007 PET was more often directly adjacent to the urinary bladder (59.3%, 16/27 cases) than was local recurrence detected on ^{68}Ga-PSMA-11 PET (48.5%, 16/33 cases). In addition, local recurrent lesions identified by PSMA-ligand imaging but not directly adjacent to the urinary bladder were closer to the bladder wall on ^{18}F-PSMA-1007 PET than on ^{68}Ga-PSMA-11 PET (mean, 2 ± 3 mm [range, 2–10 mm] vs. 4 ± 5 mm [range, 3–20 mm], respectively). Two representative examples of local recurrence on ^{18}F-PSMA-1007 PET/CT and ^{68}Ga-PSMA-11 PET/CT are presented in Supplemental Figure 1.

Lesion Validation

Validation of malignant PSMA-ligand–positive findings was available for 59 of 102 (57.8%) and 31 of 102 (30.4%) patients undergoing, respectively, ^{68}Ga-PSMA-11-PET and ^{18}F-PSMA-1007 PET with at least 1 of the following procedures: targeted radiation therapy with a consecutive PSA decline of no more than 0.2 ng/mL

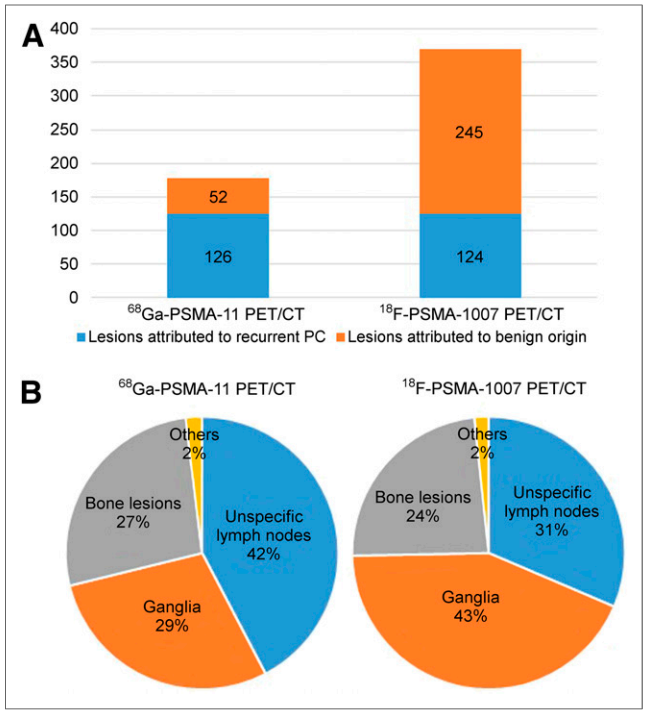

FIGURE 1. (A) Distribution of suggestive and benign lesions for all PSMA-ligand–positive lesions on ^{68}Ga-PSMA-11 PET/CT and ^{18}F-PSMA-1007 PET/CT. (B) Origin of lesions attributed to benign origin on ^{68}Ga-PSMA-11 PET/CT and ^{18}F-PSMA-1007 PET/CT.

($n = 20$ for ^{68}Ga-PSMA-11-PET and $n = 10$ for ^{18}F-PSMA-1007 PET); positive histopathology results after salvage LN dissection ($n = 5$ for ^{68}Ga-PSMA-11-PET and $n = 2$ for ^{18}F-PSMA-1007 PET); and follow-up ^{68}Ga-PSMA-11-ligand PET/CT confirming the initial suspected lesion or disappearance of suspected metastatic sites after local or systemic treatment and corresponding PSA decline ($n = 34$ for ^{68}Ga-PSMA-11-PET and $n = 19$ for ^{18}F-PSMA-1007 PET).

DISCUSSION

This exploratory matched-pair study focuses mainly on pitfalls and different interpretations of ^{68}Ga-PSMA-11 and ^{18}F-PSMA-1007 PET/CT findings. In our study, ^{18}F-PSMA-1007 PET revealed almost 5 times as many PSMA-ligand–positive findings attributed to a benign origin (mostly ganglia, unspecific LNs, and bone lesions) as did ^{68}Ga-PSMA-11 PET. Further, the detection rate for recurrent PC in ^{18}F-PSMA-1007 PET was comparable to that of ^{68}Ga-PSMA-11 PET in patients after RPE (80.4% for both ^{68}Ga-PSMA-11 and ^{18}F-PSMA-1007). However, despite the matched-pair approach with similar clinical characteristics, 2 different patient populations were compared, leading to a potential bias.

The presence of PSMA-ligand–positive benign lesions (e.g., in ganglia or healing rib fractures) has been known since the introduction of ^{68}Ga-PSMA-11 PET but has increasingly been documented in case reports or series and in review articles in recent years (*14–16*). To the best of our knowledge, our study is the first documenting the presence of a substantially higher number of PSMA-ligand–positive benign lesions on ^{18}F-PSMA-1007 PET (66.4% vs. 29.2% of all PSMA-positive lesions on ^{18}F-PSMA-1007 PET vs. ^{68}Ga-PSMA-11 PET, respectively). The presence of significantly more PSMA-ligand–positive benign lesions on

TABLE 2
Number and Percentage of Lesions Attributed to Benign Origin (Pitfall Lesions) on ^{18}F-PSMA-1007 PET and ^{68}Ga-PSMA-11 PET According to Their Origin

Parameter	^{68}Ga-PSMA-11 PET		^{18}F-PSMA-1007 PET	
	Patients	Lesions	Patients	Lesions
Pitfall lesions	34/102 (33.3%)	52	88/102 (86.3%)	245
Unspecific LN total	14/102 (13.7%)	22/52 (42.3%)	40/102 (39.2)	77/245 (31.4%)
Inguinal		2		18
Mediastinal		9		24
Hilar		8		17
Axillary		3		18
Ganglia total	12/102 (11.8%)	15/52 (28.8%)	68/102 (66.7%)	106/245 (43.3%)
Cervical		8		33
Celiac		7		64
Sacral		0		9
Bone total	15/102 (14.7%)	14/52 (26.9%)	49/102 (48.0%)	58/245 (23.7%)
Fracture		2		3
Degeneration		3		13
Unclear		3		6
Unspecific bone uptake		6		36
Others total	1/102 (1.0%)	1/52 (1.9%)	4/102 (3.9%)	4/245 (1.6%)
Unspecific uptake soft-tissue lesion*		1		2
Unclear†		—		2

*Unspecific uptake subcutaneously (n = 2) and in adenoma of adrenal gland (n = 1).
†Unclear uptake in mamma (n = 1) and kidney (n = 1).

^{18}F-PSMA-1007 PET might because the lower positron energy of ^{18}F than of ^{68}Ga improves spatial resolution on ^{18}F-PSMA-1007 PET and because ^{18}F-PSMA-1007 PET has a higher signal due to a longer half-life and higher injected activities. Finally, preclinical characteristics indicate ^{18}F-PSMA-100 to have a higher affinity and internalization rate than ^{68}Ga-PSMA-11, which could contribute to a higher signal from PSMA-expressing tissue (*17,18*).

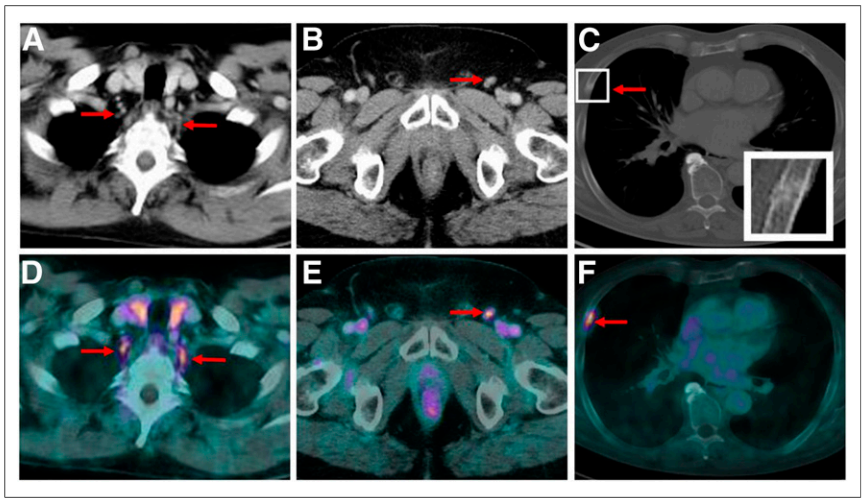

FIGURE 2. CT images (top) and ^{18}F-PSMA-1007 PET/CT images (bottom) of patient presenting with PSMA-ligand–positive, typically tear-drop–shaped cervical ganglia on both sides prevertebrally (A and D), unspecific PSMA-ligand uptake in nonenlarged left inguinal LN (B and E), and focal PSMA-ligand uptake in nondisplaced fracture of rib with corresponding fracture line and callus formation on CT images (C and F).

In ^{18}F-PSMA-1007 PET, the most prevalent pitfall lesion in our study was nonspecific physiologic radiotracer uptake in cervical, celiac, or sacral ganglia (67% vs. 12% prevalence in ^{18}F-PSMA-1007 PET vs. ^{68}Ga-PSMA PET, respectively). The initial report on PSMA-ligand uptake in celiac ganglia by Krohn et al. described visually detectable uptake in 41% of patients (*19*). Another recent publication demonstrated that visually detectable uptake of any degree in the celiac, cervical, or sacral ganglia was seen in nearly all patients. In addition, the authors demonstrated that ^{68}Ga-PSMA-11 uptake was higher in the celiac ganglia than in the cervical or sacral ganglia (*20*). Because these quantitative data are in line with our findings (Supplemental Table 1), the number of positive patients seems to be different. However, in both of the aforementioned studies, any uptake in ganglia was investigated. In our analysis, we focused only

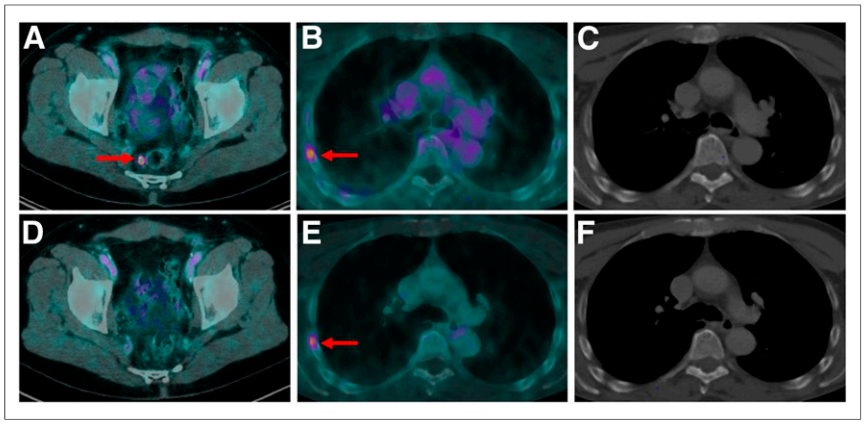

FIGURE 3. (A–C) Baseline ^{18}F-PSMA-1007 PET/CT of 65-y-old patient with BCR PC after RPE presenting with PSA value of 1.4 ng/mL. Images show single PSMA-positive LN metastasis pararectally (A, arrow). (D) This LN was removed during PSMA radioguided surgery, with subsequent PSA decline to <0.2 ng/mL and follow-up ^{18}F-PSMA-1007 PET/CT showing no PSMA ligand uptake anymore. In this patient, unspecific focal PSMA ligand uptake in right fourth rib was observed (B, arrow; SUV_{max}, 4.4) and was still present on follow-up PET/CT (E, SUV_{max}, 4.6), with no morphologic correlate on corresponding CT images (C and F).

on clearly positive cases, which could potentially lead to false findings.

The second most common pitfall lesion observed in our study was unspecific uptake in LNs (e.g., inguinal, axillary, or mediastinal). The reason for PSMA-ligand uptake in histopathologically normal LNs is not understood yet. However, immunohistochemistry studies show that PSMA is present not only in tumor-associated tissues but also in inflammation-associated neovasculature. Differentiation between suggestive and unspecific PSMA-ligand uptake in LNs is challenging but can often be resolved when looking at the shape and configuration of PSMA-positive LNs on CT images (e.g., oval vs. round configuration or presence of fatty hilum) and when reading within the clinical context (e.g., pattern of metastasis in PC, PSA level, and extent of disease). CT also plays an important role in the evaluation of benign PSMA-ligand–positive bone lesions. PSMA-ligand uptake in healing bone fracture, degenerative changes, or fibrocartilage lesions has been described before. This was also observed in our study and can be easily resolved by recognizing the respective findings on CT (e.g., fracture line or osteophytes) (*4,14,21*). However, especially on ^{18}F-PSMA-1007 PET, we observed a high amount of PSMA-ligand uptake in bone (mainly ribs) showing no clear correlate on CT images. In view of the low to intermediate (not high) uptake and the patient history, many of those were designated as unspecific uptake, with PSMA-ligand PET/CT follow-up being available for only a few of these patients. Notable, free ^{18}F cannot be regarded as a substantial issue for unspecific PSMA-ligand uptake in bones, because the mean level of free ^{18}F in all patients was only 1.8% ± 1.0% (range, 0%–3.6%).

The detection rate in our study was in line with a recent study of Giesel et al. on 251 patients with BCR after RPE undergoing ^{18}F-PSMA-1007 PET/CT (*9*). A recently published study of Rahbar et al. on ^{18}F-PSMA-1007 PET/CT in 100 patients with BCR PC observed a substantially higher detection rate of 95% (*11*). However, the median PSA level in that study was considerably higher than in our study (1.34 ng/mL [range, 0.04–41.3 ng/mL] vs. 0.87 ng/mL [range, 0.20–13.59 ng/mL], respectively).

In general, recent studies suggest a higher detection rate for ^{18}F-PSMA-1007 PET than for ^{68}Ga-PSMA-11 PET because of the higher spatial resolution of ^{18}F and the superior differentiation of ureter and bladder activity from local recurrence or locoregional LN metastases with ^{18}F-PSMA-1007. The agent is only minimally excreted via the urinary tract, posing a potential advantage (*22*). Interestingly, the results of our matched-pair study did not show a clear difference in diagnostic efficacy between ^{18}F-PSMA-1007 and ^{68}Ga-PSMA-11. Moreover, the number of local recurrent lesions was even higher in ^{68}Ga-PSMA-11 PET than in ^{18}F-PSMA-1007 PET. This difference might potentially be explained by the matched-pair approach (no double examination within 1 patient) and the limited number of patients studied. Because we matched for clinical parameters (e.g., Gleason score and primary T and N stages), the locoregional distribution of tumor lesions might not be fully matched. However, the TBR was significantly higher in ^{18}F-PSMA-1007 PET, and a considerably higher number of local recurrences directly adjacent to the urinary bladder was observed in

TABLE 3
Number and Percentage of Lesions Rated as Malignant on ^{18}F-PSMA-1007 PET and ^{68}Ga-PSMA-11 PET According to Their Origin

Parameter	^{68}Ga-PSMA-11 PET		^{18}F-PSMA-1007 PET	
	Patients	Lesions	Patients	Lesions
Total patients	82/102 (80.4%)	126	82/102 (80.4%)	124
Local recurrence	33/102 (32.4%)	33/126 (26.2%)	27/102 (26.5%)	27/124 (21.8%)
LN metastasis	51/102 (50.0%)	64/126 (50.8%)	55/102 (53.9%)	70/124 (56.5%)
Abdominopelvic		43		36
Supradiaphragmatic		21		34
Bone metastases	26/102 (25.5%)	26/126 (20.6%)	22/102 (21.6%)	22/124 (17.7%)
Other metastases	3/102 (2.9%)	3/126 (2.3%)	5/102 (4.9%)	5/124 (4.0%)

TABLE 4
Location of Unspecific Uptake in Bone Lesions on ^{18}F-PSMA-1007 PET and ^{68}Ga-PSMA-11 PET

Parameter	^{18}F-PSMA-1007 PET	^{68}Ga-PSMA-11 PET
Total lesions (*n*)	36	6
SUV_{max}	5.5 ± 1.4 (range, 3.6–10.9)	4.6 ± 1.6 (range, 3.0–7.5)
Location (*n*)		
Ribs	21	3
Spine	5	2
Pelvis	5	1
Scapula	2	—
Sternum	2	—
Femur	1	—

^{18}F-PSMA-1007 PET, supporting the benefit of low background activity in the bladder for lesion detection.

The lack of histopathologic confirmation represents a major limitation of the present study—similar to most investigations analyzing the performance of imaging in recurrent PC. However, for PSMA-ligand PET, several studies have already proven a high positive predictive value when known limitations and pitfalls are considered (*23*). However, lesion validation of malignant PSMA-ligand–positive findings was available in 58% and 30% of patients undergoing ^{68}Ga-PSMA-11 PET/CT and ^{18}F-PSMA-1007 PET/CT, respectively, which is within the range of other studies (*24,25*). Because lesions attributed to a benign origin (e.g., ganglia and unspecific LNs) are usually not validated histopathologically, corresponding CT images served as validation for approximately 80% of the benign lesions. Unfortunately, validation of unspecific PSMA-ligand uptake was available in only a minority of patients. A detailed comparison of ^{68}Ga-PSMA-11 PET and ^{18}F-PSMA-1007 PET would necessitate a head-to-head study within the same patients. For ethical reasons, this comparison needs to be performed with a prospective study and is beyond the scope of a retrospective analysis. Nevertheless, we believe that a matched-pair comparison using a variety of clinical parameters such as PSA, Gleason score, T stage, and N stage is a reasonable approach. However, further prospective studies are necessary and warranted to overcome these limitations.

CONCLUSION

A considerably higher number of visually detectable findings with increased PSMA-ligand uptake attributed to a benign origin is present on ^{18}F-PSMA-1007 PET than on ^{68}Ga-PSMA-11 PET. Therefore, especially for ^{18}F-PSMA-1007, side-by-side evaluation of PET and CT images, as well as sophisticated reader training emphasizing known pitfalls and reporting within the clinical context, are obligatory for correct and reliable PSMA-ligand PET/CT interpretation. The efficacy of detecting lesions attributed to recurrent PC was comparable in our matched-pair analysis in patients with BCR after RPE.

DISCLOSURE

Matthias Eiber received funding from SFB 824 (DFG Sonderforschungsbereich 824, project B11) from the Deutsche Forschungsgemeinschaft, Bonn, Germany, and from ABX Advanced Biochemical Compounds, Radeberg, Germany, as part of an academic collaboration. Siemens Medical Solutions (Erlangen, Germany) supported the application of Biograph mCT Flow as part of an academic collaboration. No other potential conflict of interest relevant to this article was reported.

KEY POINTS

QUESTION: In matched-pair cohorts of patients with BCR after RPE, are ^{68}Ga-PSMA-11 PET/CT and ^{18}F-PSMA-1007 PET/CT comparable in the frequency of non–tumor-related PSMA-ligand uptake and the efficacy of detection?

PERTINENT FINDINGS: The results of our retrospective matched-pair study indicate that, despite similar detection rates, ^{18}F-PSMA-1007 PET revealed almost 5 times as many PSMA-ligand–positive findings attributed to a benign origin as did ^{68}Ga-PSMA-11 PET.

IMPLICATIONS FOR PATIENT CARE: Sophisticated reader training emphasizing known pitfalls, reporting within the clinical context, and side-by-side evaluation of PET and CT images are obligatory for adequate PSMA-ligand PET/CT interpretation, especially for ^{18}F-PSMA-1007.

REFERENCES

1. Han M, Partin AW, Zahurak M, et al. Biochemical (prostate specific antigen) recurrence probability following radical prostatectomy for clinically localized prostate cancer. *J Urol.* 2003;169:517–523.
2. Briganti A, Abdollah F, Nini A, et al. Performance characteristics of computed tomography in detecting lymph node metastases in contemporary patients with prostate cancer treated with extended pelvic lymph node dissection. *Eur Urol.* 2012;61:1132–1138.
3. Perera M, Papa N, Christidis D, et al. Sensitivity, specificity, and predictors of positive ^{68}Ga-prostate-specific membrane antigen positron emission tomography in advanced prostate cancer: a systematic review and meta-analysis. *Eur Urol.* 2016;70:926–937.
4. Hofman MS, Hicks RJ, Maurer T, et al. Prostate-specific membrane antigen PET: clinical utility in prostate cancer, normal patterns, pearls, and pitfalls. *Radiographics.* 2018;38:200–217.
5. Dietlein M, Kobe C, Kuhnert G, et al. Comparison of [^{18}F]DCFPyL and [^{68}Ga]Ga-PSMA-HBED-CC for PSMA-PET imaging in patients with relapsed prostate cancer. *Mol Imaging Biol.* 2015;17:575–584.
6. Dietlein F, Kobe C, Neubauer S, et al. PSA-stratified performance of ^{18}F- and ^{68}Ga-PSMA PET in patients with biochemical recurrence of prostate cancer. *J Nucl Med.* 2017;58:947–952.
7. Giesel FL, Hadaschik B, Cardinale J, et al. F-18 labelled PSMA-1007: biodistribution, radiation dosimetry and histopathological validation of tumor lesions in prostate cancer patients. *Eur J Nucl Med Mol Imaging.* 2017;44:678–688.
8. Freitag MT, Radtke JP, Afshar-Oromieh A, et al. Local recurrence of prostate cancer after radical prostatectomy is at risk to be missed in ^{68}Ga-PSMA-11-PET of PET/CT and PET/MRI: comparison with mpMRI integrated in simultaneous PET/MRI. *Eur J Nucl Med Mol Imaging.* 2017;44:776–787.
9. Giesel FL, Knorr K, Spohn F, et al. Detection efficacy of ^{18}F-PSMA-1007 PET/CT in 251 patients with biochemical recurrence of prostate cancer after radical prostatectomy. *J Nucl Med.* 2019;60:632–638.
10. Rahbar K, Afshar-Oromieh A, Bogemann M, et al. ^{18}F-PSMA-1007 PET/CT at 60 and 120 minutes in patients with prostate cancer: biodistribution, tumour detection and activity kinetics. *Eur J Nucl Med Mol Imaging.* 2018;45:1329–1334.
11. Rahbar K, Afshar-Oromieh A, Seifert R, et al. Diagnostic performance of ^{18}F-PSMA-1007 PET/CT in patients with biochemical recurrent prostate cancer. *Eur J Nucl Med Mol Imaging.* 2018;45:2055–2061.
12. Cardinale J, Martin R, Remde Y, et al. Procedures for the GMP-compliant production and quality control of [^{18}F]PSMA-1007: a next generation radiofluorinated tracer for the detection of prostate cancer. *Pharmaceuticals (Basel).* 2017;10:E77.

13. Eder M, Neels O, Muller M, et al. Novel preclinical and radiopharmaceutical aspects of [^{68}Ga]Ga-PSMA-HBED-CC: A New PET tracer for imaging of prostate cancer. *Pharmaceuticals (Basel).* 2014;7:779–796.
14. Sheikhbahaei S, Afshar-Oromieh A, Eiber M, et al. Pearls and pitfalls in clinical interpretation of prostate-specific membrane antigen (PSMA)-targeted PET imaging. *Eur J Nucl Med Mol Imaging.* 2017;44:2117–2136.
15. Keidar Z, Gill R, Goshen E, et al. ^{68}Ga-PSMA PET/CT in prostate cancer patients: patterns of disease, benign findings and pitfalls. *Cancer Imaging.* 2018; 18:39.
16. Shetty D, Patel D, Le K, et al. Pitfalls in gallium-68 PSMA PET/CT interpretation: a pictorial review. *Tomography.* 2018;4:182–193.
17. Eder M, Schafer M, Bauder-Wust U, et al. ^{68}Ga-complex lipophilicity and the targeting property of a urea-based PSMA inhibitor for PET imaging. *Bioconjug Chem.* 2012;23:688–697.
18. Cardinale J, Schafer M, Benesova M, et al. Preclinical evaluation of ^{18}F-PSMA-1007, a new prostate-specific membrane antigen ligand for prostate cancer imaging. *J Nucl Med.* 2017;58:425–431.
19. Krohn T, Verburg FA, Pufe T, et al. [^{68}Ga]PSMA-HBED uptake mimicking lymph node metastasis in coeliac ganglia: an important pitfall in clinical practice. *Eur J Nucl Med Mol Imaging.* 2015;42:210–214.
20. Rischpler C, Beck TI, Okamoto S, et al. ^{68}Ga-PSMA-HBED-CC uptake in cervical, celiac, and sacral ganglia as an important pitfall in prostate cancer PET imaging. *J Nucl Med.* 2018;59:1406–1411.
21. Jochumsen MR, Dias AH, Bouchelouche K. Benign traumatic rib fracture: a potential pitfall on ^{68}Ga-prostate-specific membrane antigen PET/CT for prostate cancer. *Clin Nucl Med.* 2018;43:38–40.
22. Rahbar K, Weckesser M, Ahmadzadehfar H, et al. Advantage of ^{18}F-PSMA-1007 over ^{68}Ga-PSMA-11 PET imaging for differentiation of local recurrence vs. urinary tracer excretion. *Eur J Nucl Med Mol Imaging.* 2018;45:1076–1077.
23. Rauscher I, Maurer T, Beer AJ, et al. Value of ^{68}Ga-PSMA HBED-CC PET for the assessment of lymph node metastases in prostate cancer patients with biochemical recurrence: comparison with histopathology after salvage lymphadenectomy. *J Nucl Med.* 2016;57:1713–1719.
24. Eiber M, Maurer T, Souvatzoglou M, et al. Evaluation of hybrid ^{68}Ga-PSMA ligand PET/CT in 248 patients with biochemical recurrence after radical prostatectomy. *J Nucl Med.* 2015;56:668–674.
25. Rauscher I, Duwel C, Haller B, et al. Efficacy, predictive factors, and prediction nomograms for ^{68}Ga-labeled prostate-specific membrane antigen-ligand positron-emission tomography/computed tomography in early biochemical recurrent prostate cancer after radical prostatectomy. *Eur Urol.* 2018;73:656–661.